5th International Conference on Physics and Astrophysics of Quark Gluon Plasma,
February 8 - 12, 2005, Salt Lake City, Kolkata, India,
Journal of Physics: Conference Series

Strangeness and the Discovery of Quark-Gluon Plasma

Johann Rafelski[1], **Jean Letessier**[2]

[1]Department of Physics, University of Arizona, TUCSON, AZ 85718, USA

E-mail: Rafelski@Physics.Arizona.EDU

[2]Laboratoire de Physique Théorique et Hautes Energies
Université Paris 7, 2 place Jussieu, 75251 Cedex 05, France

E-mail: JLetes@LPTHE.Jussieu.FR

Abstract. Strangeness flavor yield s and the entropy yield S are the observables of the deconfined quark-gluon state of matter which can be studied in the entire available experimental energy range at AGS, SPS, RHIC, and, in near future, at the LHC energy range. We present here a comprehensive analysis of strange, soft hadron production as function of energy and reaction volume. We discuss the physical properties of the final state and argue how evidence about the primordial QGP emerges.

.

1. Introduction

The deconfined interacting quark–gluon plasma phase (QGP) is the *equilibrium* state of matter at high temperature and/or density. It is believed that this state has been present in the early Universe, 10-20μs into its evolution. The question is if, in the short time, 10^{-22}–10^{-23} s, available in a laboratory heavy ion collision experiment, the color frozen nuclear phase can melt and turn into the QGP state of matter. There is no valid first principles answer to this question available today, nor as it seems, will a first principles simulation of the dynamic heavy ion environment become available in the foreseeable future. To address this issue we study QGP experimentally, which requires development of laboratory experiments and suitable observables.

To form QGP in the laboratory we perform relativistic heavy ion collisions in which a domain of (space, time) much larger than normal hadron size is formed, in which color-charged quarks and gluons are propagating constrained by external 'frozen vacuum', which abhors color [1]. We expect a pronounced boundary in temperature and baryon density between confined and deconfined phases of matter, irrespective of the question if there is, or not, a true phase transition. We search for a boundary between phases considering the size of the interacting region and the magnitude of the reaction energy.

Detailed study of the properties of the deconfined state shows that QGP is rich in entropy and strangeness. The enhancement of entropy S arises because the color bonds are broken and gluons can be created. Enhancement of strangeness s arises because the mass threshold for strangeness excitation is considerably lower in QGP than in hadron matter. Moreover there are new mechanisms of strangeness formation in QGP involving reactions between (thermal) gluons. Thus S and s are the two elementary observables which are explored with soft hadronic probes,

for further theoretical details and historical developments see our book [2]. The numerical work presented here was carried out with the public package of programs SHARE [3]. This report is a self contained summary of our recent results, see [4, 5, 6, 7].

Entropy enhancement, observed in terms of enhanced hadron multiplicity per net charge, has been among the first indications of new physics reach of CERN-SPS experimental heavy ion program [8]. The enhancement of strange hadron production both as function of the number of participating baryons, and reaction energy has been explored in several experiments at at BNL-AGS, CERN-SPS and and BNL-RHIC. We refrain from extensive historical survey of these results and present perhaps the latest, STAR-RHIC result in Fig. 1 [9]. In this presentation one sees the yield per participant $N_{\rm part}$ divided by a reference yield obtained in pp reactions. We observe that the enhancement rises both with the strangeness content in the hadron and with the size of the reaction region, indicating that the cause of this enhancement is a increased yield of strange quarks in the source, a qualitative expectation we will address in our quantitative analysis below. The gradual increase of the enhancement over the range of $N_{\rm part}$ is an important indicator of the physics mechanisms at work. This behavior agrees with our studies of kinetic strangeness production and strangeness yield increasing with the size of the reaction region. This enhancement of strange antibaryons which demonstrates that a novel strangeness production mechanism is present has been extensively studied at SPS energy range, where it was originally discovered [10, 11].

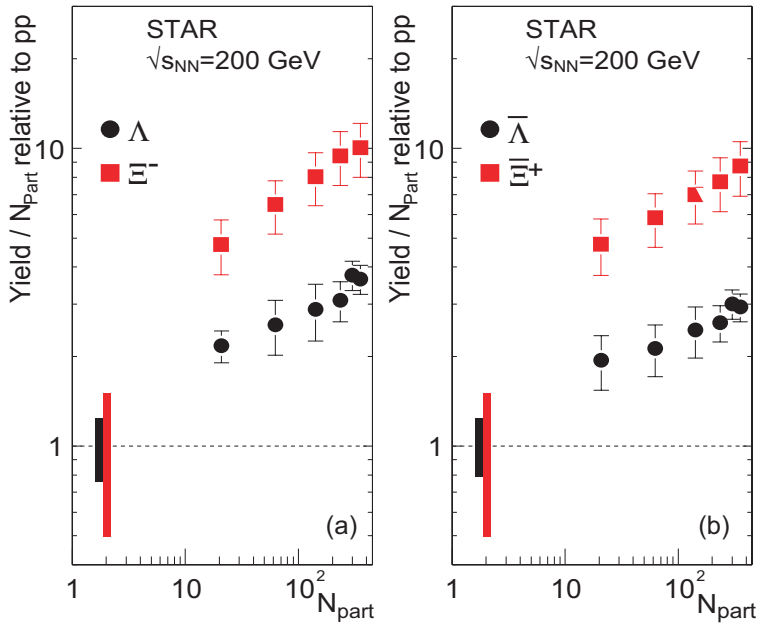

Figure 1. Yields per participant $N_{\rm part}$ relative to pp of Λ and Ξ^- on left and $\bar{\Lambda}$ and $\bar{\Xi}^+$ on right in Au+Au collisions at $\sqrt{s_{\rm NN}} = 200\,{\rm GeV}$ Error bars are statistical. Ranges for pp reference data at $N_{\rm part} = 2$ indicate the systematic uncertainty.

Further evidence for parton dynamics prior to final state hadronization is obtained from the study of strange hadron transverse energy spectrum. The identity of hyperon and antihyperon spectra in particular $\Lambda, \overline{\Lambda}$ and $\Xi, \overline{\Xi}$ implies that both strange matter and antimatter must have been produced from a common source by the same fundamental mechanism. Furthermore they were not subject to interactions in their passage through the baryon rich hadron gas present at the SPS energy range.

The $\overline{\Lambda}, \overline{\Xi}$ annihilation in baryon-rich hadron gas is strongly momentum dependent. This should deform the shape of the antihyperon spectra as compared to the spectra of hyperons. Thus symmetry of the hyperon-antihyperon spectra also implies that there was no appreciable annihilation of the $\overline{\Lambda}, \overline{\Xi}$ after their formation. The working hypothesis is therefore that hadronization of the QGP deconfined phase formed in high energy nuclear collision is direct, fast (sudden) and occurs without significant sequel interactions. That can be further tested in a study of yields and spectra of unstable resonances [12].

At RHIC the parton level dynamics is convincingly demonstrated by quark content scaling of azimuthal asymmetry of the collective flow v_2. Further evidence is derived from the consideration of quark recombination formation of hadrons from QGP. We refer to the recent comprehensive survey of the RHIC result [1], and presentations at the meeting addressing these very interesting and recent developments. We will assume in this report that the case of quark-parton dynamics prior to hadronization is convincing, and will use our analysis of soft hadron production to find the thresholds of the onset of deconfinement and to determine the properties of the deconfined fireball at the time of its breakup into hadrons.

In next section 2 we introduce the statistical hadronization method of analysis of hadron production. We discuss data analysis as function of impact parameter and energy dependence of soft hadron production in section 3. We will present both the systematics of statistical model parameters, and the associated physical properties. In section 4, we address the physical QGP signatures indicating presence of a phase boundary, giving particular attention to the explanation of the 'horn' in the K^+/π^+ ratio, and the strangeness to entropy relative yield. We discuss, in section 5, the role these results play in understanding of the phase boundary separating QGP from normal confined matter. We also discuss briefly possible new soft hadron physics at LHC.

2. Statistical hadronization model

To describe the yields of particle produced we employ the statistical hadronization model (SHM). SHM is by definition a model of particle production in which the birth process of each particle fully saturates (maximizes) the quantum mechanical probability amplitude, and thus, the relative yields are determined solely by the appropriate integrals of the accessible phase space. For a system subject to global dynamical evolution such as collective flow, this is understood to apply within each local co-moving frame.

When particles are produced in hadronization, we speak of chemical freeze-out. Hadron formation from QGP phase has to absorb the high entropy content of QGP which originates in broken color bonds. The lightest hadron is pion and most entropy per energy is consumed in hadronization by producing these particles abundantly. It is thus important to free the yield of these particles from the chemical equilibrium constraint.

The normalization of the particle yields is, aside of the freeze-out temperature T, directly controlled by the particle fugacity $\Upsilon_i \equiv e^{\sigma_i/T}$, where σ_i is particle 'i' chemical potential. Since for each related particle and antiparticle pair, we need two chemical potentials, it has become convenient to choose parameters such that we can control the difference, and sum of these separately. For example, for nucleons N, and, respectively, antinucleons $\overline{N}$ the two chemical factors are:

$$\sigma_N \equiv \mu_b + T\ln\gamma_N, \qquad \sigma_{\overline{N}} \equiv -\mu_b + T\ln\gamma_N, \tag{1}$$

$$\Upsilon_N = \gamma_N e^{\mu_b/T}, \qquad \Upsilon_{\overline{N}} = \gamma_N e^{-\mu_b/T}. \tag{2}$$

The (baryo)chemical potential μ_b, controls the baryon number, arising from the particle difference. γ_N, the phase space occupancy, regulates the number of nucleon–antinucleon pairs present. There are many different hadrons, and in principle, we could assign to each a chemical potential and then look for chemical reactions which relate these chemical potentials. However, a more direct way to accomplish the same objective consists in characterizing each particle by

the valance quark content. The relation between quark based fugacity and chemical potentials ($\lambda_{q,s} = e^{\mu_{q.,s}/T}$) and the two principal hadron based chemical potentials of baryon number and hadron strangeness $\mu_i,\ i = b, \mathrm{S}$ is:

$$\mu_b = 3\mu_q \qquad \mu_s = \frac{1}{3}\mu_b - \mu_{\mathrm{S}}, \qquad \lambda_s = \frac{\lambda_q}{\lambda_{\mathrm{S}}}. \tag{3}$$

An important (historical) anomaly is the negative S-strangeness in s-carrying-baryons. We will in general follow quark flavor and use quark chemical factors to minimize the confusion arising. In the local rest frame, the particle yields are proportional to the momentum integrals of the quantum distribution. As example, for the yield of pions π, nucleons N and antinucleons $\overline{N}$ we have:

$$\pi = V g_\pi \int \frac{d^3p}{(2\pi)^3} \frac{1}{\gamma_q^{-2} e^{E_\pi/T} - 1}, \qquad E_i = \sqrt{m_i^2 + p^2}, \quad \gamma_q^2 < e^{m_\pi/T} \tag{4}$$

$$N = V g_N \int \frac{d^3p}{(2\pi)^3} \frac{1}{\gamma_q^{-3}\lambda_q^{-3} e^{E_N/T} + 1}, \quad \overline{N} = V g_N \int \frac{d^3p}{(2\pi)^3} \frac{1}{\gamma_q^{-3}\lambda_q^{+3} e^{E_{\bar{N}}/T} + 1}. \tag{5}$$

There are two types of chemical factors γ_i and μ_i, and thus two types of chemical equilibriums. These are shown in table 1. The absolute equilibrium is reached when the phase space occupancy approaches unity, $\gamma_i \to 1$. The distribution of flavor (strangeness) among many hadrons is governed by the relative chemical equilibrium.

Table 1. Four quarks s, $\overline{s}$, q, and $\overline{q}$ require four chemical parameters; right: name of the associated chemical equilibrium

γ_i	controls overall abundance of quark ($i = q, s$) pairs	Absolute chemical equilibrium
λ_i	controls difference between quarks and antiquarks ($i = q, s$)	Relative chemical equilibrium

In order to arrive at the full particle yield, one has to be sure to include all the hadronic resonances which decay feeding into the yield considered, *e.g.*, the decay $K^* \to K + \pi$ feeds into K and π yields. The contribution is sensitive to temperature at which these particles are formed. Inclusion of the numerous resonances constitutes a book keeping challenge in study of particle multiplicities, since decays are contributing at the 50% level to practically all particle yields. A public statistical hadronization program, SHARE (Statistical HAdronization with REsonances) has simplified this task considerably [3].

The resonance decay contribution is dominant for the case for the pion yield. This happens even though each resonance contributes relatively little in the final count. However, the large number of resonances which contribute compensates and the sum of small contributions competes with the direct pion yield. For the more heavy hadrons, generally there is a dominant contribution from just a few, or even from a single resonance. The exception are the $\Omega, \overline{\Omega}$ which have no known low mass resonances, and also ϕ – the known resonances are very heavy and very few.

A straightforward test of sudden hadronization and the SHM is that within a particle 'family', particle yields with same valance quark content are in relation to each other well described by integrals of relativistic phase space. The relative yield of, *e.g.*, $K^*(\bar{s}q)$ and $K(\bar{s}q)$ or Δ and N are

controlled by the particle masses m_i, statistical weights (degeneracy) g_i and the hadronization temperature T. In the Boltzmann limit one has (star denotes the resonance):

$$\frac{N^*}{N} = \frac{g^* m^{*\,2} K_2(m^*/T)}{g\, m^2 K_2(m/T)}. \tag{6}$$

Validity of this relation implies insensitivity of the quantum matrix element governing the coalescence-fragmentation production of particles to intrinsic structure (parity, spin, isospin), and particle mass. The measurement of the relative yield of hadron resonances is a sensitive test of the statistical hadronization hypothesis and lays the foundation to the application of the method in data analysis.

The method available to measure resonance yields depends in its accuracy significantly on the the precise nature of the hadronization process: the resonance yield is derived by reconstruction of the invariant mass of the resonance from decay products energies E_i and momenta p_i. Should the decay products of resonances after formation rescatter on other particles, then often their energies and momenta will change enough for the invariant mass to fail the acceptance conditions set in the experimental analysis. Generally, the rescattering effect depletes more strongly the yields of shorter lived resonances , as a greater fraction of these will decay shortly after formation, when elastic scattering of decay products on other produced particles is possible.

We further hear often the argument that the general scattering process of hadrons in matter can form additional resonance states. In our opinion, the loss of observability (caused by *any* scattering of *any* of the decay products is considerably greater than a possible production gain. The loss of resonance yield provides additional valuable information about the freeze-out conditions (temperature and time duration)[12].

3. Phase thresholds: volume and energy dependence

3.1. Statistical model parameters

In order to explore the properties of the fireball at hadronization as function of the volume at the top RHIC energy $\sqrt{s_{NN}} = 200\,\mathrm{GeV}$ Au–Au, we study the 11 centrality bins in which the $\pi^{\pm}, \mathrm{K}^{\pm}, p$ and $\bar{p}$ rapidity yields dN/dy for $y_{\mathrm{CM}} = 0$ have been recently presented, see table I and table VIII in Ref. [13]. These 6 particle yields and their ratios change rapidly. On the other hand, the additional two experimental results, the STAR $\mathrm{K}^*(892)/\mathrm{K}^-$ [14], and ϕ/K^- [15] show little centrality dependence.

In addition, three supplemental constraints help to determine the best fit:
A) strangeness conservation, *i.e.*, the (grand canonical) count of s quarks in all hadrons equals such $\bar{s}$ count for each rapidity unit;
B) the electrical charge to net baryon ratio in the final state is the same as in the initial state;
C) the ratio $\pi^+/\pi^- = 1. \pm 0.02$, which helps constrain the isospin asymmetry.
This last ratio appears redundant, as we already independently use the yields of π^+ and π^-. These yields have a large systematic error and do not constrain their ratio well, and thus the supplemental constraint is introduced, since SHARE allows for the isospin asymmetry effect. The 7 SHM parameters (volume per unit of rapidity dV/dy, temperature T, four chemical parameters $\lambda_q, \lambda_s, \gamma_q, \gamma_s$ and the isospin factor λ_{I3} are in this case studied in a systematic fashion as function of impact parameter using 11 yields and/or ratios and/or constraints, containing one (pion ratio) redundancy.

Although the number of degrees of freedom in such analysis is small, the χ^2 minimization yielding good significance is easily accomplished, showing good consistency of the data sample. The resulting statistical parameters are shown in Fig. 2, as function of participant number. We show on left results for the full non-equilibrium model allowing $\gamma_q \neq 1, \gamma_s \neq 1$ (full circles, blue) and semi-equilibrium setting $\gamma_s = 1$ (open circles, red). From top to bottom the (chemical) freeze-out temperature T, the occupancy factors γ_q, γ_s/γ_q and together in the bottom panel the

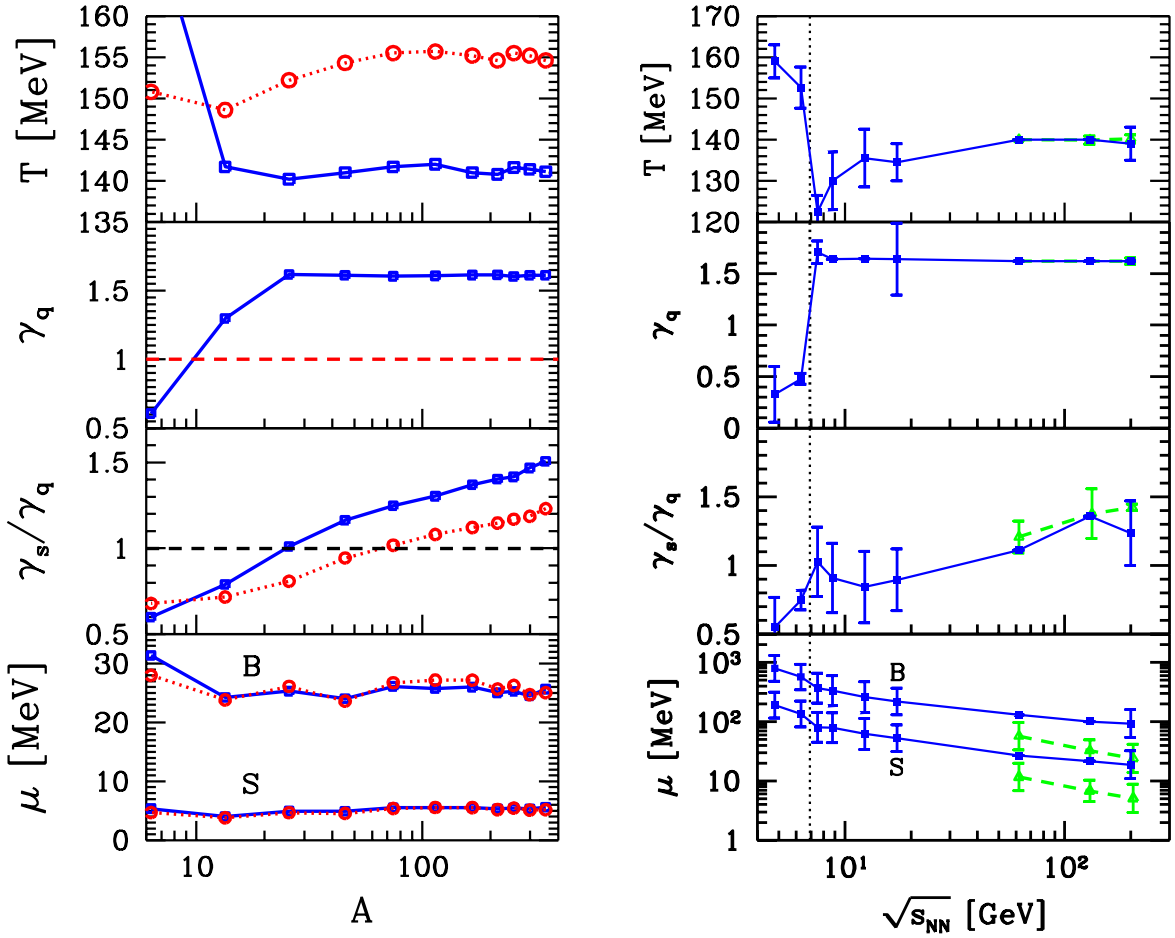

Figure 2. From top to bottom: temperature T, light quark phase space occupancy γ_q, the ratio of strange to light quark phase space occupancies γ_s/γ_q and the chemical potentials (B for baryochemical μ_B and S for strangeness μ_S) The lines guide the eye. Left: as function of centrality *i.e.* impact parameter dependence presented as dependence on inelastic (wounded) participant number A. Right: energy $\sqrt{s_{\rm NN}}$-dependence. Note that the results at RHIC (left side and the two highest energies in green on right) apply to central rapidity region dN/dy study, while the AGS/SPS energy results are obtained from total yields and are extrapolated to the top Brahms result at RHIC.

baryon μ_B and hyperon μ_S chemical potentials. On left, in Fig. 2, we present the results for the centrality dependence, as function of participant number, on right as function of energy.

To study the energy dependence, we must assemble several different experimental results from different facilities and experiments [6]. The results of this extensive analysis are shown on right hand side in Fig. 2. We note that when we are able to consider the total particle abundances, the number of participating nucleons is a tacit fit parameter. The lowest energy result is from our AGS study [4], the SPS data we used are from NA49 energy dependence exploration at the CERN-SPS [11, 16]. These results are for the total particle yields. The highest energy two results are based on studies of RHIC data at 130 and 200 GeV at central rapidity and address the dN/dy particle yields, with the highest point corresponding to the results presented at greatest centrality on the left hand side in Fig. 2.

There are several relevant features in Fig. 2. We see on left, that, for $A > 20$, there is no centrality dependence in freeze-out temperature T and chemical potentials $\mu_{B,S}$ (up to the variation which can be associated with fluctuation in the data sample). However, there is a change in values of the chemical potentials with reaction energy. This is result of rapidly decreasing baryon density, which due to reduced stopping is distributed over a wider range of rapidity as the reaction energy increases.

The middle sections, in Fig. 2, address the phase space occupancies which were obtained in terms of hadron particle yields. The quark-side occupancy parameters could be considerably different, indeed as model studies show, a factor 2 lower at the discussed conditions [2]: the hadron side phase space size is in general different from the quark-side phase space, since the particle degeneracies, particle spectra are quite different. We see similar behavior of γ_q as of T both for volume (that is, 'wounded' participant number A) and energy dependence seen in Fig. 2: the two lowest energy bins (top AGS and lowest SPS energy) deviate from the behavior seen at all other energies, as do the bins with $A < 20$. γ_s/γ_q as function of centrality rises steadily indicating longer lifespan of the fireball with increasing size. As function of energy, γ_s/γ_q reaches a plateau at 30 AGeV, with further rise only seen in the central rapidity results at RHIC. We note that, in our analysis, there is no saturation of the γ_s as we approach the most central reactions. This is inherent in the data we consider which includes the yields of ϕ, and K^*. This result is consistent with the implication that strangeness is not fully saturated in the QGP source, though it appears over-saturated when measured in the hadron phase space.

The deviation at the most peripheral centrality bins and at lowest reaction energy from trends set by other results could be an indication of the change in the reaction mechanism. As a threshold of centrality and/or energy are crossed a relatively small value of $\gamma_q \simeq 0.5$ grows rapidly to the maximum allowed by pion condensation condition, $\gamma_q \simeq e^{m_\pi/2T} \simeq 1.6$. This behavior signals a transformation of a chemically under-saturated phase of matter into something novel, where chemical equilibration is easy, and results in hadronization in a over-saturated phase of matter.

Independent of the chemical (non-)equilibrium assumption, the baryochemical potential $\mu_B = 25 \pm 1$ MeV is seen across 10 centrality bins. Similarly, we find strangeness chemical potential $\mu_S = 5.5 \pm 0.5$ MeV (related to strange quark chemical potential $\mu_s = \mu_B/3 - \mu_S$). The most notable variation, in Fig. 2, is the gradual increase in strangeness phase space occupancy γ_s/γ_q and thus strangeness yield with collision centrality. This effect was predicted and originates in an increasing lifespan of the fireball [17]. The over-saturation of the phase space has been also expected due to both, the dynamics of expansion [18], and/or reduction in phase space size as a parton based matter turns into HG [19]. This latter effect is also held responsible for the saturation of light quark phase space $\gamma_q \to e^{m_\pi/2T}$. A systematic increase of γ_s with collision centrality has been reported for several reaction energies [20].

3.2. Hadronization Temperature

Let us now discuss more in depth the magnitude of the hadronization temperature which at high energy/central collisions we find at $T = 140$ MeV. Some prefer the statistical hadronization to occur at higher temperature, perhaps as high as$T = 175$ MeV, a point argued at this meeting in great detail by Dr. Peter Braun-Münzinger. In his presentation we heard that he believes that the lattice results will reach to such high temperature near to $mu_{\rm B} = 0$ and this is where one should expect to see hadronization We disagree with both claims. For one,

We note that *chemical equilibrium QCD lattice* [21] results are mature and yield $T = 163 \pm 2$ MeV when extrapolated to physical quark mass scale. This result is in a very good agreement with the prior work on 2 and 3 flavor QCD which brackets this result by $T_{n_f=2,3} = T \pm 10$ MeV [22]. Moreover, the heavy ion collisions present a highly dynamical environment and one has to pay tribute to this especially regarding the value of hadronization temperature. For this

reason we do not expect to find that the observed hadronization condition $T(\mu_{\rm B})$ will line up with the phase boundary curve obtained in study of a statistical system in thermodynamic limit on the lattice:

a) Dependence on parton collective flow:
A widely discussed effect which displaces the hadronization condition from the phase boundary is the expansion dynamics of the fireball. When the collective flow occurs at parton level, the color charge flow, like a wind, pushes out the vacuum [23], adding to thermal pressure a dynamical component. This can in general lead to supercooling and a sudden breakup of the fireball. We find that this can reduce the effective hadronization temperature by up to 20 MeV [24].

b) Dependence on quark chemical equilibration:
Lattice result have been discussed for 2-flavor lattice QCD at corresponding to $\gamma_q = 1, \gamma_s = 0$ (called) and for 2+1 flavor, corresponding to $\gamma_q = \gamma_s = 1$. While the precise nature of the phase limit is still under study it appears that for 2-flavor case the phase boundary temperature rises by about 7-10 MeV compared to the 2+1 case. We refer to the recent review of lattice QCD for further details [25]. Similarly the phase limit in pure gauge case corresponding in loose sense to $\gamma_q = \gamma_s = 0$ was seen near or even above $T = 200$ MeV.

These results do suggest that presence and the number of quarks matters regarding the precise location of the phase boundary and its nature. Its importance could be greatly enhanced, should the over-saturation of quark phase space have the same effect as would additional quark degrees of freedom. These are known to cause even for $\mu_{\rm B} = 0$ the conversion of the phase crossover into a 1st-order phase transition which would, with these additional degrees of freedom, be expected at just the temperature we find in the SHM analysis.

We can be nearly sure that the chemical conditions matter and can displace the transition temperature. Because the degree of equilibration in the QGP depends on the collision energy, as does the collective expansion velocity, we cannot at all expect a simple hadronization scheme appropriate for the hadronization of nearly adiabatically expanding Universe.

Leaving this issue we note that, in the data analysis assuming chemical equilibrium, we find $T = 155 \pm 8$ MeV for the chemical equilibrium and strangeness non-equilibrium freeze-out, see Fig. 2. The error is our estimate of the propagation of the systematic data error, combined with the fit uncertainty; the reader should note that the error comparing centrality to centrality is negligible. The freeze-out temperature is for the semi-equilibrium and equilibrium model about 10% greater than the full chemical non-equilibrium freeze-out.

This result for T, in the equilibrium case, is in mild disagreement (1.5 s.d.) with earlier equilibrium fits [26, 27]. This, we believe, is due to some differences in data sample used, specifically, the hadron resonance production results used provide a very strong constraint for the fitted temperature, and more complete treatment by SHARE of hadron mass spectrum.

Interestingly, it seems that the general consensus about the chemical equilibrium best analysis result is in gross disagreement with the results advanced at this meeting by Dr. Peter Braun-Münzinger.

3.3. Physical Properties of the Fireball

We now turn our attention to the physical properties of the hadronizing fireball obtained summing individual contributions made by made of each of the hadronic particles produced. Often particles observed experimentally dominate (*e.g.* pions dominate pressure, kaon strangeness yield etc). However, it is important to include in this yields of particles predicted in terms of the SHM fit to the available results. Again, on left in Fig. 3. we show the behavior as function of impact parameter and on right as function of energy. From top to bottom we show the pressure P, energy density ϵ, entropy density σ, and the dimensionless ratio $\epsilon/T\sigma = E/TS$. All contributions are evaluated using relativistic expression, see [2].

When we fitted particle rapidity yields, the global fitted yield normalization factor is

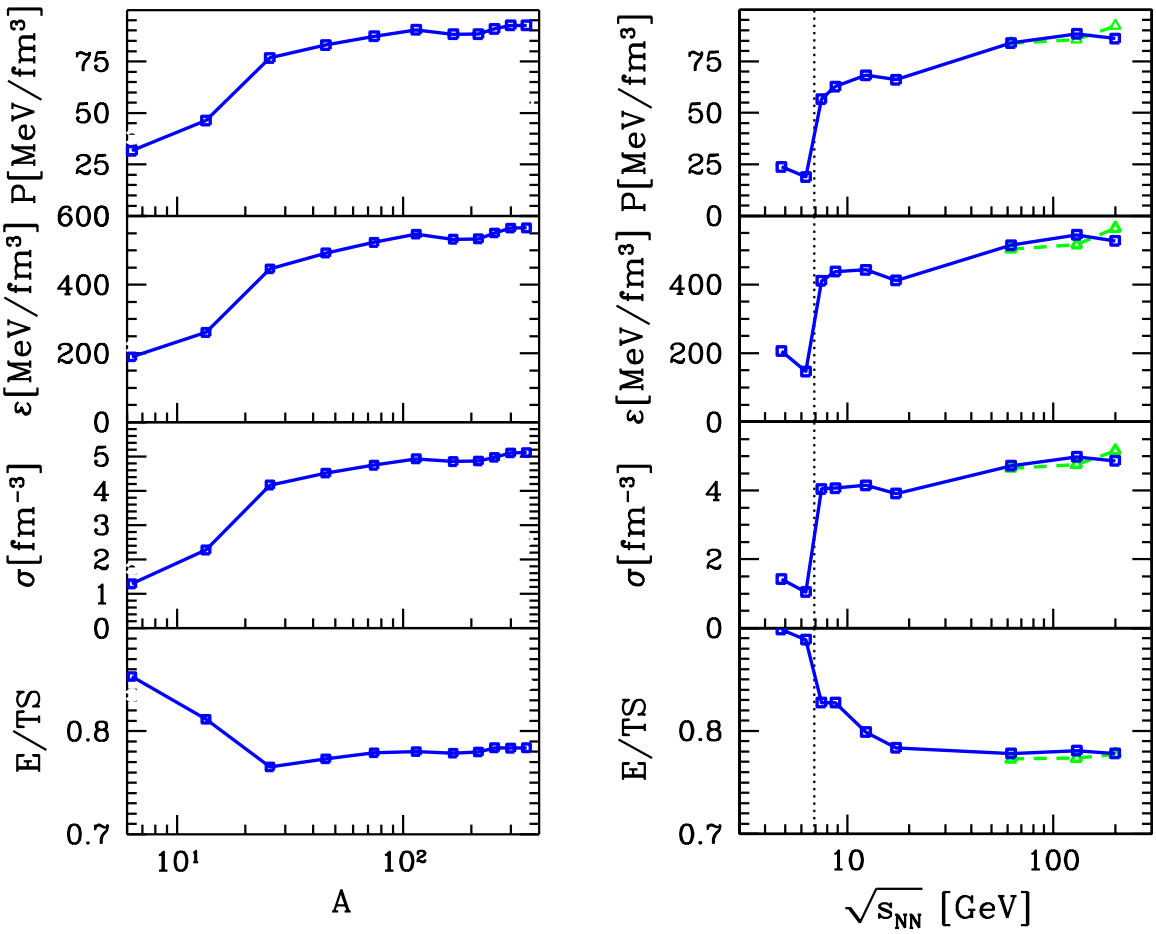

Figure 3. From top to bottom: pressure P, energy density $\epsilon = E/V$, entropy density S/V and E/TS; Left: as a function of centrality, Right as function of reaction energy. The results on left are for central rapidity, and on right are for the full phase space coverage, except for the high energy RHIC results (open triangles, green) which are for central rapidity. Open circles on left apply to the semi-non-equilibrium analysis with $\gamma_q = 1, \gamma_s \neq 1$, all other results are for the chemical nonequilibrium analysis.

$dV(A)/dy$, for total particle yields it is V which is also a function of centrality trigger. When we consider ratios of two bulk properties e.g. E/TS, the results are in general smoother indicating cancellation in the error propagating from the fit. The overall error is of the magnitude of the particle yield, for example pressure is dominated by pions and hence its precision is limited by this error. However, on left, the point-to-point error is minimal as the systematic error is common. On right, the absolute error matters as the fluctuations in the results presented show.

We note, in Fig. 3, that as the reaction energy passes the volume threshold $A = 20$ and even more so, the energy threshold $6.26\,\mathrm{GeV} < \sqrt{s_{\mathrm{NN}}} < 7.61\,\mathrm{GeV}$ the hadronizing fireball becomes much denser. The entropy density jumps by factor 3–4, and the energy and baryon number density by a factor 2–3. The hadron pressure jumps up from $P = 25\,\mathrm{MeV/fm^3}$ initially by factor 2 and ultimately more than factor 3. There is a gradual increase of $P/\epsilon = 0.115$ at low reaction energy to 0.165 at the top available energy. It is important to note that exactly the same behavior of the fireball physical properties arises both as function of reaction volume and reaction energy. This is the case for both the physical properties and the statistical parameters.

We believe that this shows a common change in the physical state created as function of energy available and reaction volume.

4. Search for an Energy Threshold

4.1. Kaon to pion ratio

One of the most interesting questions is if there is an energy threshold for the formation of a new state of matter. An important observable of the deconfined phase of matter is aside of strangeness, the high entropy content, which is arising from broken color bonds. The observable for both is the $\mathrm{K}^+/\pi^+ \propto \bar{s}/\bar{d}$ yield ratio [28]. This ratio has been studied experimentally [11] and a pronounced horn structure arises. We can describe this structure in our study of the particle yields only within the chemical non-equilibrium model. Although this change is associated a rather sudden modification of chemical conditions in the dense matter fireball, this effect is caused by two distinct phenomena: the rapid rise in strangeness $\bar{s}$ production below, and a rise in the antiquark $\bar{d}$ yield above a energy reaction threshold.

The measured K^+/π^+ ratio by NA49 is shown at top left of Fig. 4, where for comparison we also show the *pp* results. On right top, we present our results reduced to the correct relative scale, both for the total yield ratio for the AGS–RHIC energy range, and for the central rapidity results from RHIC. The solid line guides the eye to the fit results we obtained. To show that the K^+/π^+ ratio drop is due to a decrease in baryon density which leads to rise in the $\bar{d}$ yield, we show in bottom section of Fig. 4, the nearly baryon density independent K/π double ratio ratio Eq. (7), on left as function of $\sqrt{s_{\mathrm{NN}}}$, and on right as function of centrality of the reaction for $\sqrt{s_{\mathrm{NN}}} = 200$ GeV:

$$\frac{K}{\pi} = \sqrt{\frac{K^+}{\pi^+}\,\frac{K^-}{\pi^-}}. \tag{7}$$

Both upper and lower portion of Fig. 4 are also drawn on same relative scale.

Seen how the horn specifically arises in the one K^+/π^+, one can wonder if this is really a physical effect and how, in qualitative terms, a parameter γ_q, which controls the light quark yield, can help explain the horn structure seen in top of Fig. 8. We observe that this horn structure in the K^+/π^+ ratio traces out the final state valance quark ratio $\bar{s}/\bar{d}$, and in language of quark phase space occupancies γ_i and fugacities λ_i, we have:

$$\frac{\mathrm{K}^+}{\pi^+} \rightarrow \frac{\bar{s}}{\bar{d}} \propto F(T)\left(\frac{\lambda_s}{\lambda_d}\right)^{-1}\frac{\gamma_s}{\gamma_d} = F(T)\left(\sqrt{\lambda_{I3}}\frac{\lambda_s}{\lambda_q}\right)^{-1}\frac{\gamma_s}{\gamma_q}. \tag{8}$$

In chemical equilibrium models $\gamma_s/\gamma_q = 1$, and the K^+/π^+ ratio and its horn must arise solely from the variation in the ratio λ_s/λ_q and the change in temperature T which both are usually smooth function of reaction energy. The isospin factor λ_{I3} is insignificant in this consideration.

As collision energy is increased, increased hadron yield leads to a decreasing $\lambda_q = e^{\mu_{\mathrm{B}}/3T}$. We recall the smooth decrease of μ_{B} with reaction energy seen in bottom panel in Fig. 2. The two chemical fugacities λ_s and λ_q are coupled by the condition that the strangeness is conserved. This leads to a smooth λ_s/λ_q. The chemical potential effect is suggesting a smooth increase in the K^+/π^+ ratio.

For the interesting range of freeze-out temperature, $F(T)$ is a smooth function of T. Normally, one expects that T increases with collision energy, hence on this ground as well we expect an monotonic increase in the K^+/π^+ ratio as function of reaction energy. With considerable effort, one can arrange the chemical equilibrium fits to bend over to a flat behavior at $\sqrt{s^{\mathrm{cr}}_{\mathrm{NN}}}$. It is quasi impossible to generate the horn with chemical equilibrium model. To accomplish this, an additional parameter appears necessary, capable to change rapidly when hadronization conditions change. This is γ_q. It presence also allows T to vary in non-monotonic fashion, as is seen in Fig. 2.

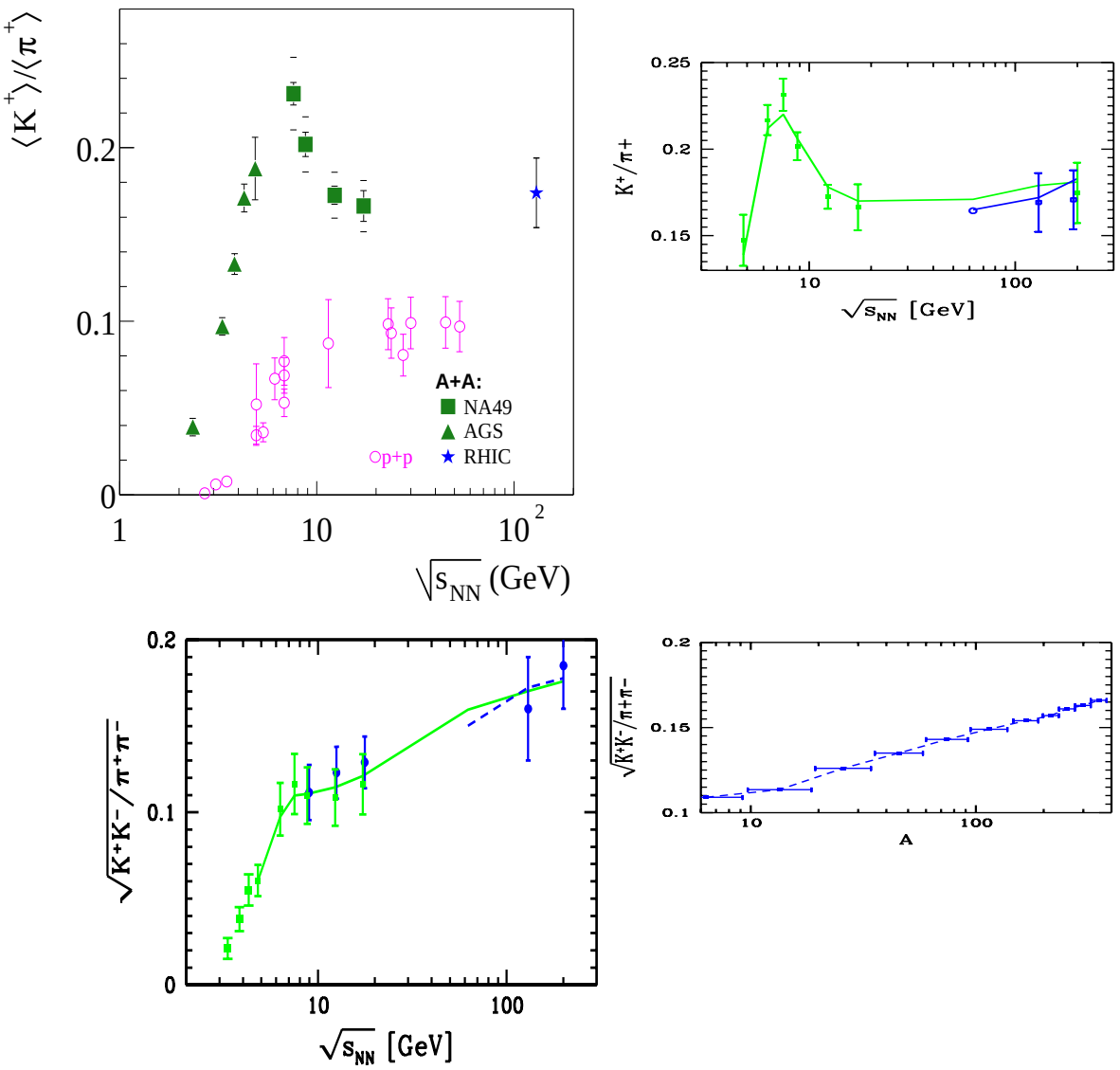

Figure 4. Top: Total yield-ratio of yields of K^+/π^+ for nuclear (filled symbols, green) and elementary interactions (open symbols, violet); (courtesy of NA49 collaboration [29]). On right: a fit to this K^+/π^+ ratio using SHM, at high energy also for central rapidity RHIC, line guides the eye between the fitted values. Bottom: the K/π ratio for nuclear collisions, squares on left (green): full phase space on left, circles (blue) are central rapidity results, left as function of collision energy and right as function of participant number at $\sqrt{s_{\rm NN}} = 200$ GeV.

4.2. QGP degrees of freedom and s/S ratio

The full SHM is capable to describe the data, and we now show that it can pinpoint the properties of the phase of matter that was created early on in the reaction. To see this we consider what we learn from the final state data about strangeness and entropy production. For this purpose we consider both the specific per baryon and per entropy yield of strangeness. In addition, we look at the cost in thermal energy to make strangeness. All these quantities are nearly independent of the dynamics of hadronization, since they are related to processes occurring early on, 'deep' inside the collision region, and long before hadronization.

In the QGP, the dominant entropy production occurs during the initial glue thermalization, and the thermal strangeness production occurs in parallel and/or just a short time later [30].

The entropy production occurs predominantly early on in the collision during the thermalization phase. Strangeness production by gluon fusion is most effective in the early, high temperature environment, however it continues to act during the evolution of the hot deconfined phase until hadronization [31]. Both strangeness and entropy are nearly conserved in the evolution towards hadronization and thus the final state hadronic yield analysis value for s/S is closely related to the thermal processes in the fireball at $\tau \simeq 1$–2 fm/c. We believe that for reactions in which the system approaches strangeness equilibrium in the QGP phase, one can expect a prescribed ratio of strangeness per entropy, the value is basically the ratio of the QGP degrees of freedom.

We estimate the magnitude of s/S deep in the QGP phase, considering the hot stage of the reaction. For an equilibrated non-interacting QGP phase with perturbative properties:

$$\frac{s}{S} \equiv \frac{\rho_{\rm s}}{\sigma} = \frac{(3/\pi^2)T^3(m_s/T)^2K_2(m_s/T)}{(32\pi^2/45)T^3 + n_{\rm f}[(7\pi^2/15)T^3 + \mu_q^2 T]} = \frac{0.027}{1 + 0.054(\ln\lambda_q)^2}\,. \tag{9}$$

Here, we used for the number of flavors $n_{\rm f} = 2.5$ and $m_s/T = 1$. We see that the result is a slowly changing function of λ_q; for large $\lambda_q \simeq 4$, we find at modest SPS energies, the value of s/S is reduced by 10%. Considering the slow dependence on $x = m_s/T \simeq 1$ of $W(x) = x^2K_2(x)$ there is minor dependence on the much less variable temperature T.

The dependence on the degree of chemical equilibration which dominates is easily obtained separating the different degrees of freedom:

$$\frac{s}{S} = 0.027\frac{\gamma_s^{\rm QGP}}{0.38\gamma_{\rm G}^{\rm QGP} + 0.12\gamma_s^{\rm QGP} + 0.5\gamma_q^{\rm QGP} + 0.054\gamma_q^{\rm QGP}(\ln\lambda_q)^2}\,. \tag{10}$$

We assume that the interaction effects are at this level of the discussion canceling. Seen Eq. (10) we expect to see a gradual increase in s/S as the QGP source of particles approaches chemical equilibrium with increasing collision energy and/or increasing volume.

We repeat that it is important to keep in mind that this ratio s/S is established early on in the reaction, the above relations, and the associated chemical conditions we considered, apply to the early hot phase of the fireball. At hadron freeze-out the QGP picture used above does not apply. Gluons are likely to freeze faster than quarks and both are subject to much more complex non-perturbative behavior. However, the value of s/S is nearly preserved from the hot QGP to the final state of the reaction.

How does this simple prediction compare to experiment? Given the statistical parameters, we can evaluate the yields of particles not yet measured and obtain the rapidity yields of entropy, net baryon number, net strangeness, and thermal energy, both for the total reaction system and also for the central rapidity condition, also as function of centrality. In passing, we note that, in the most central reaction bin at RHIC-200, $dB/dy \simeq 15$ baryons per unit rapidity interval, implying a rather large baryon stopping in the central rapidity domain.

The rise of strangeness yield with centrality is faster than the rise of baryon number yield: $(ds/dy)/(dB/dy) \equiv s/B$ is seen in the top left panel in Fig. 5. The solid (blue) lines are for the chemical nonequilibrium central rapidity yields of particles at RHIC-200. Solid (green) lines, on right, are for total hadron yields and thus total yields of the considered quantities, *e.g.* strangeness, entropy. For the most central head-on reactions, we reach at RHIC-200 $s/B = 9.6 \pm 1$.

In the middle panel in Fig. 5 we compare strangeness with entropy production s/S, which we just evaluated theoretically. Again, on left, as function of participant number A at RHIC-200 and, on right, for the total reaction system for the most central 5-7% reactions. On left, we see a smooth transition from a flat peripheral behavior where $s/S \lesssim 0.02$ to smoothly increasing s/S reaching $s/S \simeq 0.028$ in most central reactions. This indicates that even at RHIC-200 for the more central reactions some new mechanisms of strangeness production becomes activated. On

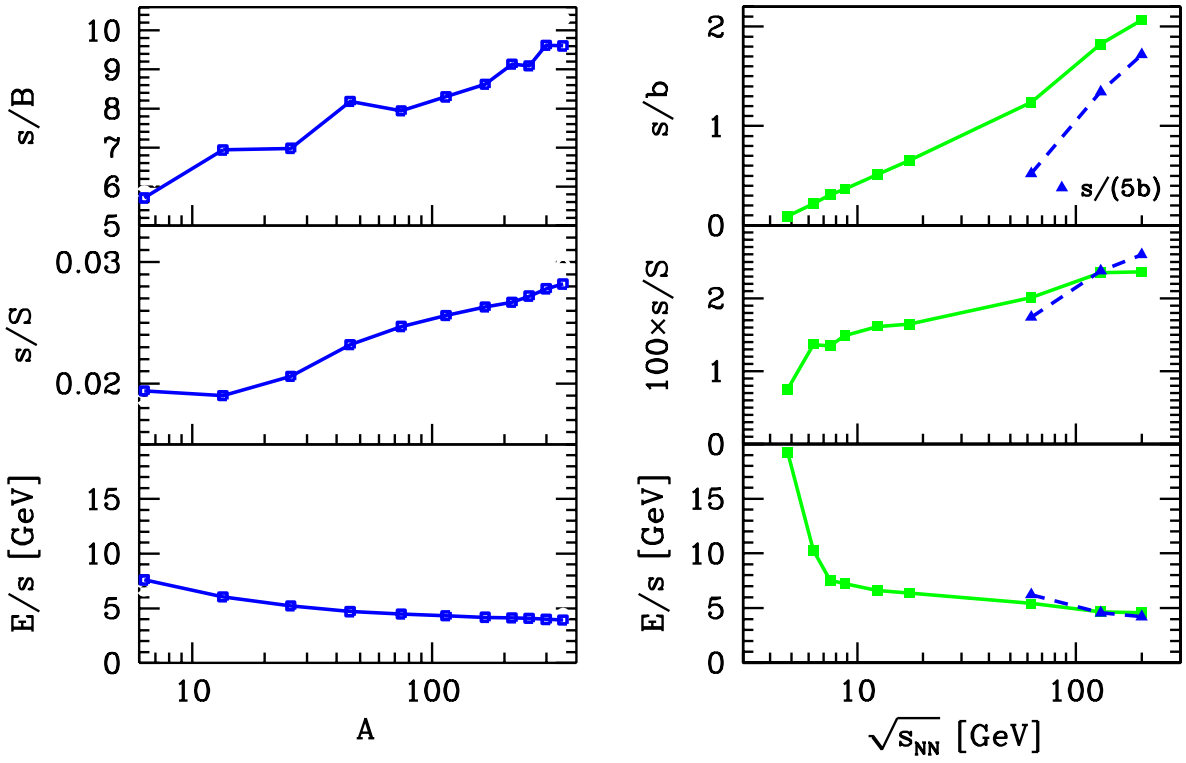

Figure 5. Strangeness per net baryon s/B, strangeness per entropy s/S, and $E_{\rm th}/s$ the thermal energy cost to make strangeness. Left: as a function of centrality, Right as function of reaction energy. The results on right include the central rapidity conditions at RHIC energies (dashed, blue) lines. The actual results are the symbols, the lines guide the eye.

right, we see that the change on s/S is much more drastic as function of reaction energy. After an initial rapid rise the further increase occurs beyond the threshold energy at slower pace.

In the bottom panel, on left, we see the thermal energy cost $E_{\rm th}/s$ of producing a pair of strange quarks as function of the size of the participating volume (*i.e.* A) This quantity shows a smooth drop which can be associated with transfer of thermal energy into collective transverse expansion after strangeness is produced. Thus, it seems that the cost of strangeness production is independent of reaction centrality. The result is different when we consider $\sqrt{s_{\rm NN}}$ dependence of this quantity, see bottom panel on right. There is a very clear change in the energy efficiency of making strangeness at the threshold energy. We will return to discuss possible reaction mechanisms below.

5. Final remarks

5.1. Phase boundary and hadronization conditions

The chemical freeze-out conditions we have determined presents, in the T–$\mu_{\rm B}$ plane, a more complex picture than naively expected, see Fig. 6. Considering results shown in Fig. 2, we are able to assign to each point in the T–$\mu_{\rm B}$ plane the associate value of $\sqrt{s_{\rm NN}}$. The RHIC dN/dy results are to outer left. They are followed by RHIC and SPS $N_{4\pi}$ results. The dip corresponds to the 30 and 40 AGeV SPS results. The top right is the lowest 20 AGeV SPS and top 11.6 AGeV AGS energy range. To guide the eye, we have added two lines connecting the fit results. We see that the chemical freeze-out temperature T rises for the two lowest reaction energies 11.6

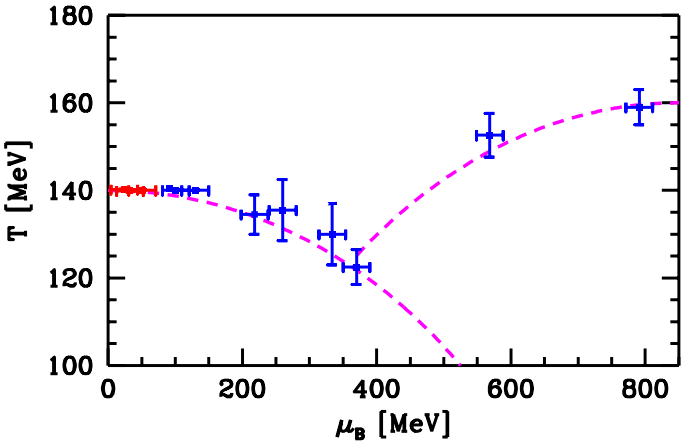

Figure 6. T–$\mu_{\rm B}$ plane with points obtained in the SHM fit.

and 20 A GeV to near the Hagedorn temperature, $T = 160$ MeV, of boiling hadron matter.

Once the chemical non-equilibrium is allowed for, the data fit turns to be much more precise, and the picture of the phase boundary with smaller 'measurement' error reveal a much more complex structure, and contains physics details prior analysis based on a rudimentary model could not uncover. The shape of the hadronization boundary, shown in Fig. 6 in the T–$\mu_{\rm B}$ plane, is the result of a complex interplay between the dynamics of heavy ion reaction, and the properties of both phases of matter, the inside of the fireball, and the hadron phase we observe. The dynamical effect, capable to shift the location in temperature of the expected phase boundary is due to the expansion dynamics of the fireball which occurs at parton level, and effects of chemical nonequilibrium, see subsection 3.2 for full discussion.

Possibly, not only the location, but also the *nature* of the phase boundary can be modified by variation of γ_i. We recall that for the 2+1 flavor case, there is a critical point at finite baryochemical potential with $\mu_{\rm B} \simeq 350$ MeV [21]. For the case of 3 massless flavors, there can be a 1st order transition at all $\mu_{\rm B}$ [22, 33, 34]. Considering a classical particle system, one easily sees that an over-saturated phase space, *e.g.*, with $\gamma_q = 1.6$, $\gamma_s \geq \gamma_q$ for the purpose of the study of the phase transition acts as being equivalent to a system with 3.2 light quarks and 1.6 massive (strange) quarks present in the confined hadron phase.

Considering the sudden nature of the fireball breakup seen in several observables [1], we conjecture that the hadronizing fireball leading to $\gamma_s > \gamma_q = 1.6$ super-cools and experiences a true 1st order phase boundary corresponding also at small $\mu_{\rm B}$. The system we observe in the final state prior to hadronization is mainly a quark–antiquark system with gluons frozen in prior expansion cooling of the QCD deconfined parton fluid. The quark dominance is necessary to understand *e.g.* how the azimuthal asymmetry v_2 varies for different particles [35].

These quarks and antiquarks have, in principle, at that stage a significant thermal mass. The evidence for this is seen in Fig. 3 in its two bottom panels, showing the dimensionless variable E/TS. The energy end entropy per particle of non-relativistic and semi-relativistic classical particle gas comprising both quarks and antiquarks is (see section 10, [2]):

$$\frac{E}{N} \simeq m + 3/2\,T + \ldots, \quad \frac{S}{N} \simeq 5/2 + m/T + \ldots, \qquad \frac{E}{TS} \simeq \frac{m/T + 3/2}{m/T + 5/2}\,. \tag{11}$$

It is thus possible to interpret the fitted value $E/TS \to 0.78$ in terms of a quark matter made of particles with $m \propto aT$, $a = 2$ which is close to what is expected based on thermal QCD [36].

5.2. Looking forward to LHC

We expect considerably more violent transverse expansion of the fireball of matter created at LHC. The kinetic energy of this transverse motion must be taken from the thermal energy of the expanding matter, and ultimately this leads to local cooling and thus a reduction in the number of quarks and gluons. The local entropy density decreases, but the expansion assures that the total entropy still increases. Primarily, gluons are feeding the expansion dynamics, while strange quark pair yield, being weaker coupled remain least influenced by this dynamics. Model calculations show that this expansion yields an increase in the final QGP phase strangeness occupancy γ_s [32]. This mechanism, along with the required depletion of the non-strange degrees of freedom, in the feeding of the expansion, assures an increase in the K/π ratio given the nearly 30-fold increase of collision energy.

Depending on what we believe to be a valid hadronization temperature for a fast transversely expanding fireball, the possible maximal enhancement in the K/π ratio may be in the range of a factor 2–3. Perhaps even more interesting than the K/π ratio enhancement would be the enhancement anomaly in strange (antibaryon) yields. With $\gamma_s \gg 1$, we find that the more strange baryons and antibaryons are more abundant than the more 'normal' species. Specifically of interest would be $(\Omega^- + \overline{\Omega}^+)/(h^+ + h^-)$, $(\Xi^- + \overline{\Xi}^+)/(h^+ + h^-)$, and $2\phi/(h^+ + h^-)$ which should show a major, up to an order of magnitude shift in relative production strength. Detailed predictions for the yields of these particles require considerable extrapolation of physics conditions from the RHIC to LHC domain and this work is in progress [37].

Ultimately, strange s, and $\bar{s}$ quarks can exceed in abundance the light quark component, in which case we would need to rethink in much more detail the distribution of global particle yield. The ratios of neutral and charged hadrons would undergo serious change.

Regarding charm, we note that situation will not become as severe. Given the large charm quark mass, we expect that most of charm quark yield is due to first hard interactions of primary partons. For this reason, the yield of strange and light quarks, at time of hadronization, exceeds by about a factor 100 or more that of charm at central rapidity. Thus, even though charm phase space occupancy at hadronization may largely exceed the chemical equilibrium value, seen the low hadronization temperature, *e.g.*, $m_c/T \simeq 10$, it takes a factor $\gamma_c \simeq e^{10}/10^{1.5} = 700$ to compensate hadron yield suppression due to the high charm mass. Said differently, while strange quarks can compete in abundance with light quarks for $m_s/T \simeq 1$, charm (and heavier) flavor(s) will remain suppressed, in absolute yield, at the temperatures we can make presently in laboratory experiments.

5.3. Highlights

We have shown that strangeness, and entropy, at SPS and RHIC are well developed tools allowing the detailed study of hot QGP phase. Our detailed discussion of hadronization analysis results has further shown that a systematic study of strange hadrons fingerprints the properties of a new state of matter at point of its breakup into final state hadrons.

We have shown that it is possible to describe the 'horn' in the K^+/π^+ hadron ratio within the chemical non-equilibrium statistical hadronization model. We have shown that appearance of this structure is related to a rapid change in the properties of the hadronizing matter. Of most theoretical relevance and interest are the implications of non-equilibrium hadronization on the possible change in the location and *nature* of the phase boundary.

In summary, we have presented interpretation of the experimental soft hadron data production and discussed the production of strangeness and entropy that this analysis infers. We have seen, in quantitative way, how the relative strangeness and entropy production in most central high energy heavy ion collisions agrees with quark-gluon degree of freedom counting in hot primordial matter where the values of these quantities have been established.

Acknowledgments
Work supported in part by a grant from: the U.S. Department of Energy DE-FG02-04ER4131. LPTHE, Univ. Paris 6 et 7 is: Unité mixte de Recherche du CNRS, UMR7589. JR thanks Bikash Sinha and Jan-e Alam and the organizers of the 5th International Conference on Physics and Astrophysics of Quark Gluon Plasma, February 8 — 12, 2005 Salt Lake City, Kolkata, India for their kind hospitality. Dedicated to Professor Bikash Sinha on occasion of his 60th anniversary.

References

[1] Assessments by the RHIC experimental collaborations: *Hunting the Quark Gluon Plasma: results from the first 3 years at RHIC* BNL-73847-2005 Formal Report, April 18, 2005, to appear in Nucl. Phys. A (2005).
[2] J. Letessier and J. Rafelski, *Hadrons and quark - gluon plasma* Cambridge Monogr. Part. Phys. Nucl. Phys. Cosmol. **18** 1-397 (2002) (Cambridge, UK, 2002). Available on line to read freely with WIN and MAC platforms at http://site.ebrary.com/pub/cambridgepress/Doc?isbn=0521385369
[3] G. Torrieri, W. Broniowski, W. Florkowski, J. Letessier and J. Rafelski, [arXiv:nucl-th/0404083], Computer Physics Communications in press, see: www.physics.arizona.edu/˜torrieri/SHARE/share.html
[4] J. Letessier, J. Rafelski and G. Torrieri, "Deconfinement energy threshold: Analysis of hadron yields at 11.6-A-GeV," arXiv:nucl-th/0411047.
[5] J. Rafelski, J. Letessier and G. Torrieri, "Centrality dependence of bulk fireball properties at RHIC," arXiv:nucl-th/0412072.
[6] J. Letessier and J. Rafelski, "Hadron production and phase changes in relativistic heavy ion collisions," arXiv:nucl-th/0504028.
[7] J. Rafelski and J. Letessier, Acta Phys. Polon. B **34**, 5791 (2003) [arXiv:hep-ph/0309030]; and J. Phys. G **30** (2004) S1 [arXiv:hep-ph/0305284].
[8] J. Letessier, A. Tounsi, U. W. Heinz, J. Sollfrank and J. Rafelski, Phys. Rev. Lett. **70**, 3530 (1993).
[9] H. Caines [STAR Collaboration], J. Phys. G **31**, S1057 (2005).
[10] G. E. Bruno [NA57 Collaboration], J. Phys. G **30**, S717 (2004) [arXiv:nucl-ex/0403036].
[11] M. Gazdzicki *et al.* [NA49 Collaboration], J. Phys. G **30**, S701 (2004) [arXiv:nucl-ex/0403023].
[12] J. Rafelski, J. Letessier and G. Torrieri, Phys. Rev. C **64**, 054907 (2001) [Erratum-ibid. C **65**, 069902 (2002)].
[13] S. S. Adler *et al.* [PHENIX Collaboration], Phys. Rev. C **69**, 034909 (2004) [arXiv:nucl-ex/0307022].
[14] H. B. Zhang [STAR Collaboration], "Delta, K* and rho resonance production and their probing of freeze-out dynamics at RHIC,", poster presentation at QM2004, Oakland, January 2004 [arXiv:nucl-ex/0403010]; J. Adams [STAR Collaboration], [arXiv:nucl-ex/0412019], Phys. Rev. C. (2005) in press.
[15] J. Adams *et al.* [STAR Collaboration], Phys. Lett. B **612**, 181 (2005) [arXiv:nucl-ex/0406003].
[16] M. Gazdzicki, Commented compilation of NA49 results, private communication.
[17] J. Letessier, A. Tounsi and J. Rafelski, Phys. Lett. B **389** (1996) 586.
[18] J. Rafelski and J. Letessier, Phys. Lett. B **469**, 12 (1999) [arXiv:nucl-th/9908024].
[19] J. Rafelski and J. Letessier, Nucl. Phys. A **702**, 304 (2002) [arXiv:hep-ph/0112027].
[20] B. Kampfer, J. Cleymans, P. Steinberg and S. Wheaton, Heavy Ion Phys. **21**, 207 (2004).
[21] Z. Fodor and S. D. Katz, JHEP **0404**, 050 (2004) [arXiv:hep-lat/0402006].
[22] F. Karsch, Nucl. Phys. A **698**, 199 (2002) [arXiv:hep-ph/0103314].
[23] T. Csorgo and J. Zimanyi, Heavy Ion Phys. **17**, 281 (2003) [arXiv:nucl-th/0206051].
[24] J. Rafelski and J. Letessier, Phys. Rev. Lett. **85**, 4695 (2000) [arXiv:hep-ph/0006200].
[25] F. Karsch and E. Laermann, arXiv:hep-lat/0305025. In R.C. Hwa, et al.: Quark gluon plasma III (2004) pp 1-59 (World Scientific, Singapore).
[26] P. Braun-Munzinger, K. Redlich and J. Stachel, [arXiv:nucl-th/0304013], and references therein.
[27] W. Broniowski, W. Florkowski and B. Hiller, Phys. Rev. C **68**, 034911 (2003) [arXiv:nucl-th/0306034].
[28] N. K. Glendenning and J. Rafelski, Phys. Rev. C **31**, 823 (1985).
[29] M. vanLeeuwen, Compilation of NA49 results as function of collision energy. Private communication (2003).
[30] J. Alam, B. Sinha and S. Raha, Phys. Rev. Lett. **73**, 1895 (1994).
[31] J. Rafelski and B. Müller, *Phys. Rev. Lett* **48**, 1066 (1982); **56**, 2334E (1986).
[32] J. Rafelski and J. Letessier, *Phys. Lett.* B **469**, 12 (1999).
[33] A. Peikert, F. Karsch, E. Laermann and B. Sturm, Nucl. Phys. Proc. Suppl. **73**, 468 (1999) .
[34] C. Bernard *et al.* [MILC Collaboration], Phys. Rev. D **71**, 034504 (2005) .
[35] H. Z. Huang and J. Rafelski, AIP Conf. Proc. **756**, 210 (2005) [arXiv:hep-ph/0501187].
[36] P. Petreczky, F. Karsch, E. Laermann, S. Stickan and I. Wetzorke, Nucl. Phys. Proc. Suppl. **106**, 513 (2002).
[37] J. Rafelski and J. Letessier, "Soft hadron relative multiplicites at LHC" (in preparation).